J|A|C|S
ARTICLES
Published on Web 04/27/2002

Synthesis and Properties of Water-Soluble Gold Colloids Covalently Derivatized with Neutral Polymer Monolayers

Claire Mangeney,[†] Fabien Ferrage,[‡] Isabelle Aujard,[†] Valérie Marchi-Artzner,[§] Ludovic Jullien,*[,†] Olivier Ouari,[||] El Djouhar Rékaï,[||] André Laschewsky,*[,||,#] Inger Vikholm,[⊥] and Janusz W. Sadowski*[,⊥]

Contribution from the Département de Chimie CNRS UMR 8640, Ecole Normale Supérieure, 24 rue Lhomond, F-75231 Paris Cedex 05, France, Département de Chimie CNRS UMR 8642, Ecole Normale Supérieure, 24 rue Lhomond, F-75231 Paris Cedex 05, France, Laboratoire de Chimie des Interactions Moléculaires, Collège de France, 11, Place Marcelin Berthelot, F-75005 Paris, France, Département de Chimie, Université Catholique de Louvain, Place L. Pasteur, 1, B-1348 Louvain-la-Neuve, Belgium, and VTT Automation, Sensing Materials, P.O. Box 13042, FIN-33101 Tampere, Finland

Received March 27, 2001

Abstract: Citrate-capped gold nanoparticles as well as planar gold surfaces can be efficiently grafted with a covalently attached polymer monolayer a few nanometers thick, by simple contact of the metal surface with dilute aqueous solutions of hydrophilic polymers that are end-capped with disulfide moieties, as shown by UV/vis absorption, dynamic light scattering, and surface plasmon resonance studies. The hydrophilic polymer-coated gold colloids can be freeze-dried and stored as powders that can be subsequently dissolved to yield stable aqueous dispersions, even at very large concentrations. They allow for applying filtrations, gel permeation chromatography, or centrifugation. They do not suffer from undesirable nonspecific adsorption of proteins while allowing the diffusion of small species within the hydrogel surface coating. In addition, specific properties of the original hydrophilic polymers are retained such as a lower critical solution temperature. The latter feature could be useful to enhance optical responses of functionalized gold surfaces toward interaction with various substrates.

Introduction

In recent years, inorganic nanoparticles have attracted considerable attention.[1] Among them, silver, gold, and copper colloids have been the major focus of interest because of their unique optical properties determined by the collective oscillations of electron density termed plasmons.[2] The efficiency for the absorption and scattering of light by metal nanoparticles can surpass that of any molecular chromophore.[3] In addition, both absorption and scattering properties can be considerably altered by surface modification, or by electronic coupling between individual nanoparticles. Together with an exceptional resistance to photodegradation, such favorable optical features are stimulating the development of new applications in analytical chemistry and in photophysics, making metal colloids attractive components for diagnostic, electronic, and photonic devices.

Control over size and chemical stability of the metal particles are important prerequisites for many potential applications. From the latter point of view, gold colloids are probably the most attractive. Several different routes to stable gold colloids have been developed over the past few years. The classical citrate method is often used to generate gold colloids.[4] New synthetic methods have been introduced to obtain gold nanoparticles with a better control over size and shape so as to make different particle geometries accessible in the 1−100 nm range.[5] For many purposes, it is important to stabilize the metal colloids against aggregation or/and to derivatize them with various molecules. Recently, long chain thiols were used both for stabilization and for derivatization during biphasic syntheses of small gold colloids. The resulting colloidal materials are obtained as stable concentrated solutions or as powders that can be redispersed after the addition of organic solvents.[6] Besides the ease of synthesis, these thiol-modified gold colloids behave as robust large molecules that are amenable to characterization by a variety of analytical methods.[7]

* To whom correspondence should be addressed. E-mail: Ludovic.Jullien@ens.fr.
[†] UMR 8640, Ecole Normale Supérieure.
[‡] UMR 8642, Ecole Normale Supérieure.
[§] Collège de France.
[||] Université Catholique de Louvain.
[⊥] VTT Automation.
[#] New address: Fraunhofer-Institute of Applied Polymer Research, Geiselbergstrasse 69, D-14476 Golm, Germany.

(1) (a) Elghanian, R.; Storhoff, J. J.; Mucic, R. C.; Letsinger, R. L.; Mirkin, C. A.; *Science* **1997**, *277*, 1078−1081. (b) Bruchez, M., Jr.; Moronne, M.; Gin, P.; Weiss, S.; Alivisatos, P. A. *Science* **1998**, *281*, 2013−2016. (c) Schmid, G.; Chi, L. F. *Adv. Mater*. **1998**, *10*, 515−526. (d) Volokitin, Y.; Sinzing, J.; de Jongh, L. J.; Schmid, G.; Moiseev, I. I. *Nature* **1996**, *384*, 621−623.
(2) Kreibig, U.; Vollmer, M. *Optical Properties of Metal Clusters*; Springer Series in Material Science, 25; Springer-Verlag: Berlin, 1995.
(3) Bohren, C. F.; Hoffman, D. R. *Absorption and Scattering of Light by Small Particles*; John Wiley and Sons: New York, 1998.
(4) Frens, G. *Nature (London)* **1973**, *241*, 20−22.
(5) Pileni, M. P. *J. Phys. Chem*. **1993**, *97*, 6961−6973.

In contrast, chemical functionalization of gold nanoparticles preformed in aqueous solution has often resulted in stability problems; colloid aggregation is indicated by a red-shift of the plasmon band.[8] This problem is traditionally overcome by adding large amounts of polymeric stabilizers that exhibit a low and unspecific affinity for the particle surface.[9] However, stabilizers at such large concentrations can severely interfere with a subsequent surface functionalization. One approach to simultaneously solve both the issues of colloidal stability and of colloid derivatization consists of using hydrophilic polymeric functionalizable stabilizers that are covalently grafted on the nanoparticle surfaces. When biological molecules or environments are involved, the polymeric stabilizers should be compatible with biomedical requirements.[10] This approach can also be applied to other types of gold surfaces that are extensively used in diagnostic techniques using SPR devices, quartz crystal microbalances, or impedance measurements.[11] Polysaccharides have been extensively investigated for this purpose. Nevertheless, both the grafting on gold and the activation of the polymer backbone for further derivatizations require multistep approaches. In addition, the building of the final metal/hydrogel surface coating composite obeys a strict hierarchy, the biomolecules being incorporated in the last step. As steric hindrance hampers the access to the colloid surface, the maximal amount of biomolecules that can be fixed is severely limited.

We report here on gold colloids which are covalently derivatized with hydrophilic polymer brushes bearing terminal disulfide groups and being compatible with biological applications. The modified nanoparticles can be stored for long periods in the dry state and are easily redispersed in aqueous solutions where they give stable solutions, even at the highest concentration. Simple direct mixing of the gold colloids with polymer solutions results in grafting onto the metal surface. A priori, the chemistry involved in the grafting-on-gold step is (i) compatible with other types of nanoparticles,[12] and (ii) mild enough to allow the fixation onto gold to take place even after the polymer has been modified with fragile fragments such as biomolecules. This paper describes the preparation and some properties of gold colloids surface-derivatized by hydrophilic polymers. Further functionalization with substrates of biological interest will be published in a forthcoming paper.

Results and Discussion

Design, Synthesis, and Characterization of the Hydrophilic Polymers. Hydrophilic polymers were designed to satisfy two types of demands. On one hand, the polymers must dispose of anchor groups that bind selectively to gold. Also, they must afford rather thin layers on gold, that is, not thicker than 100 nm, because of the limited penetration depth of the wave probing the medium from gold surfaces. On the other hand, concerning possible biomedical or analytical applications, the polymers must be resistant to hydrolysis as well as to biological degradation, for example, by enzymes or by microorganisms. Additionally, they must minimize unspecific adsorption (in particular of biological molecules), while allowing the fixation of a sufficient quantity of selectively reacting groups for further derivatization. Moreover, the polymers should also enable easy handling and storage, as well as the regeneration of the gold surfaces for sensing applications. In this context, we prepared hydrogel surface coatings by a "grafting-to" strategy.[13] Nonionic hydrophilic polymers bearing hydroxyl groups were grafted to gold surfaces using disulfide anchors. The resulting monolayers can be derivatized for the specific recognition of analytes, either using unsymmetrical bifunctional linker groups or directly when the polymer bears already "activated" sites (Figure 1).

We focused on polymers based on the monomers: *N*-[tris(hydroxymethyl)methyl]acrylamide **1** and *N*-(isopropryl)acrylamide **2**. Monomer **1** gives polymers that are nonionic, very hydrophilic,[14] biocompatible,[15] and inert to biological fouling. Moreover, the high number of primary hydroxyl groups enables facile post-functionalization.[16] Monomer **2** produces a thermoresponsive homopolymer in aqueous solution, exhibiting a conformational collapse above a lower critical solution temperature (LCST).[17] Importantly, this thermal transition is affected by various factors (cosolvent, pH, ionic strength, internal balance between hydrophilic and hydrophobic groups in the polymer, ...).[16,17] These features made us wonder whether the interaction between an analyte and a polymer containing monomer **2** could induce a local polymer collapse of the hydrogel so as to amplify the sensitivity of the detection technique. The hydrogel surface coatings would then be no more an inert matrix, but would become an "active" component. In the present study, we wanted to investigate in particular (i) whether thermal transitions could be observed close to gold surfaces, and (ii) whether these transitions could significantly change the observed signals.

Two series of poly(acrylamide)s were synthesized. In the first series, the disulfide-functionalized diazo initiator **S** was employed to incorporate a metal-anchoring moiety in the hydrophilic polymers (Scheme 1).[18] Thus, polymers **P1S** and

(6) (a) Bartz, M.; Küther, J.; Nelles, G.; Weber, N.; Seshadriet, R.; Tremel, W. *J. Mater. Chem.* **1999**, *9*, 1121−1127. (b) Liu, J.; Ong, W.; Roman, E.; Lynn, M. J.; Kaifer, A. E. *Langmuir* **2000**, *16*, 3000−3002. (c) Thomas, K. G.; Kamat, P. V. *J. Am. Chem. Soc.* **2000**, *122*, 2655−2656. (d) Quaroni, L.; Chumanov, G. *J. Am. Chem. Soc.* **1999**, *121*, 10642−10643. (e) Boal, A. K.; Rotello, V. M. *J. Am. Chem. Soc.* **2000**, *122*, 734−735. (f) Hostetler, M. J.; Wingate, J. E.; Zhong, C. J.; Harris, J. E.; Vachet, R. W.; Clark, M. R.; Londono, J. D.; Green, S. J.; Stokes, J. J.; Wignall, G. D.; Glish, G. L.; Porter, M. D.; Evans, N. D.; Murray, R. W. *Langmuir* **1998**, *14*, 17−30. (g) Liu, J.; Mendoza, S.; Roman, E.; Lynn, M. J.; Xu, R.; Kaifer, A. E. *J. Am. Chem. Soc.* **1999**, *121*, 4304−4305.

(7) (a) Hostetler, M. J.; Murray, R. W. *Curr. Opin. Colloid Interface Sci.* **1997**, *2*, 42−50 and references therein. (b) Hostetler, M. J.; Green, S. J.; Stokes, J. J.; Murray, R. W. *J. Am. Chem. Soc.* **1996**, *118*, 4212−4213. (c) Loweth, C. J.; Caldwell, W. B.; Peng, X.; Alivisatos, A. P.; Shultz, P. G. *Angew. Chem., Int. Ed.* **1999**, *38*, 1809−1812. (d) Johnson, S. R.; Evans, S. D.; Mahon, S. W.; Ulman, A. *Langmuir* **1997**, *13*, 51−57. (e) Brust, M.; Walker, M.; Bethell, D.; Schiffrin, D. J.; Whyman, R. *J. Chem. Soc., Chem. Commun.* **1994**, 801−802. (f) Brust, M.; Fink, J.; Bethell, D.; Schiffrin, D. J.; Kiely, C. *J. Chem. Soc., Chem. Commun.* **1995**, 1655−1656. (g) Sarathy, K. V.; Kulkarni, G. U.; Rao, C. N. R. *J. Chem. Soc., Chem. Commun.* **1997**, 537−538. (h) Mirkin, C. A.; Letsinger, R. L.; Mucic, R. C.; Storhoff, J. J. *Nature* **1996**, *382*, 607−609.

(8) Fujiwara, A.; Yanagida, S.; Kamat, P. V. *J. Phys. Chem. B* **1999**, *103*, 2589−2591.

(9) Sato, T.; Ruch, R. *Stabilization of Colloidal Dispersions by Polymer Adsorption*; Surfactant Science Series, 9; Marcel Dekker: New York, 1980.

(10) (a) Chen, C. W.; Takezako, T.; Yamamoto, K.; Serizawa, T.; Akashi, M.; *Colloids Surf., A* **2000**, *169*, 107. (b) Wang, C.; Stewert, R. J.; Kopecek, J. *Nature* **1999**, *397*, 417−420. (c) Winnik, F. M. *Macromolecules* **1990**, *23*, 233−242.

(11) Sackmann, E.; Tanaka, M. *Trends Biotechnol.* **2000**, *18*, 58−64. Pei, R.; Xiurong Yang, X.; Wang, E. *Talanta* **2000**, 5*3*, 481−488.

(12) See, for instance: Kumar, A.; Mandale, A. B.; Sastry, M. *Langmuir* **2000**, *16*, 9299−9302.

(13) For a "grafting-from" approach, see: Laschewsky, A.; Ouari, O.; Mangeney, C.; Jullien, L. *Macromol. Symp.* **2001**, *164*, 323−340.

(14) (a) Köberle, P.; Laschewsky, A.; van den Boogaard, D. *Polymer* **1992**, *33 (19)*, 4029−4039. (b) Saito, N.; Sugawara, T.; Matsuda, T. *Macromolecules* **1996**, *29*, 313−319.

(15) (a) Barthélemy, P.; Maurizis, J. C.; Lacombe, J. M.; Pucci, B. *Bioorg. Med. Chem. Lett.* **1998**, *8*, 1559−1562. (b) Contino, C.; Maurizis, J. C.; Pucci, B.; *Macromol. Chem. Phys.* **1999**, *200*, 1351−1355.

(16) Laschewsky, A.; Rekaï, E. D.; Wischerhoff, E. *Macromol. Chem. Phys.* **2001**, *202*, 276−286.

(17) Schild, H. G.; Tirell, D. A. *J. Phys. Chem.* **1990**, *94*, 4352−4356.

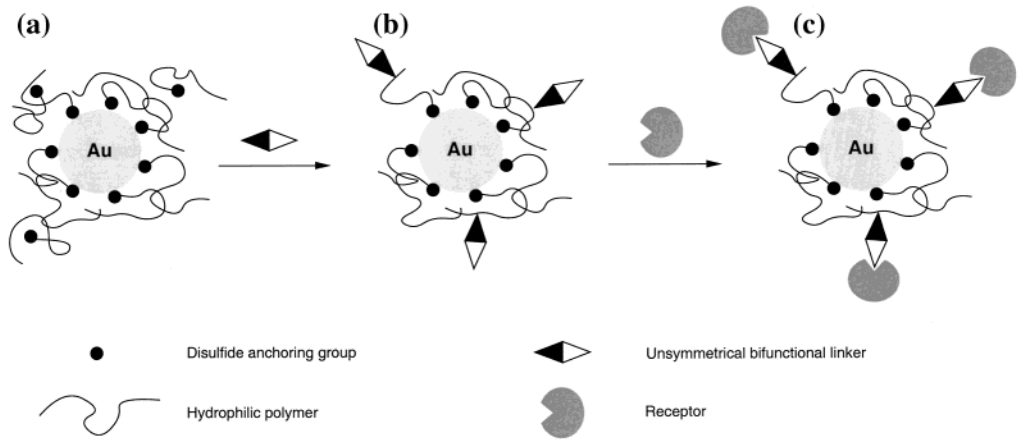

Figure 1. Stepwise "grafting-to" derivatization of gold surfaces. (a) Fixation of the polymer with disulfide anchoring groups. (b) Activation of the polymer by unsymmetrical bifunctional linker groups. (c) Functionalization of the polymer by receptors. Step b is omitted when "activated" polymers are used.

Scheme 1. Chemical Formula of the Polymers Employed

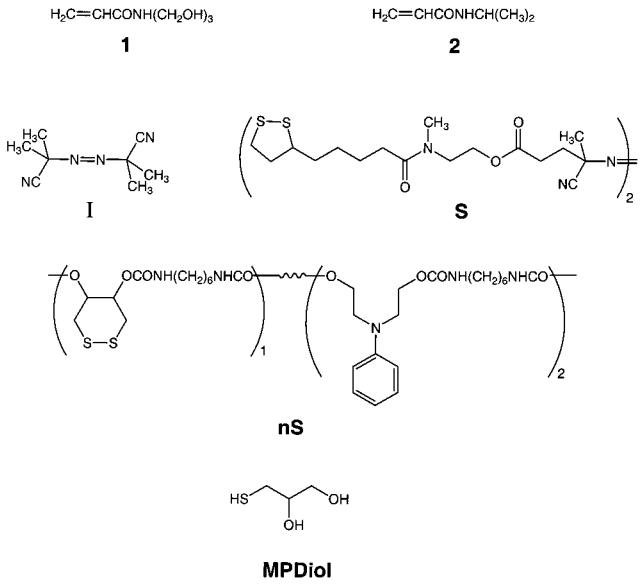

P2S were obtained by free radical homopolymerization of **1**, or by copolymerization of a 95:5 (mol/mol) mixture of **2** and **1**, respectively. For comparison, the analogous reference compounds **P1I** and **P2I** were prepared using a standard initiator, AIBN. **P1nS** was prepared by polymerization of **1** using the multifunctional photoinitiating system of oligo(oxy-1,2-dithiane 4,5-diyl-oxycarbonyliminohexamethylene imino carbonyl)-*co*-(oxy dimethylene *N*-phenylimino-dimethylene-oxycarbonyl iminohexamethylene iminocarbonyl) **nS** together with a water-soluble thioxanthone, presumably resulting in starlike polymers. Bearing more disulfide moieties than **P1S**, **P1nS** allows one to evaluate the significance of the number of anchoring groups for our purpose.

Water is the only common standard solvent for the polymers investigated. We could not determine the molar masses by size exclusion chromatography, due to the partial adsorption of the polymers on the column material. Therefore, we measured the self-diffusion coefficients in water by ^{1}H NMR translational self-diffusion measurements, to estimate the magnitude of the

Table 1. Characterization of the Polymers **P1I**, **P2I**, **P1S**, **P2S**, **P1nS** by ^{1}H NMR Translational Self-Diffusion Measurements in Water at 298 K

polymer **P**	$D_t \times 10^{11}$ ($m^2\ s^{-1}$)	$R \pm 20\%$ (nm)[a]	$N \pm 20\%$[b]	$\langle MW \rangle \pm 20\%$[c]	$\langle r \rangle \pm 20\%$ (nm)[d]
P1I	3.5 ± 0.5	6.2	210	37 000	31
P2I	9.7 ± 0.1	2.2	40	4500	16
P1S	6.9 ± 0.1	3.2	70	12 000	22
P2S	8.1 ± 0.1	2.7	55	6000	17
P1nS	8.5 ± 0.3	2.6	50	9000	20

[a] Hydrodynamic radii R calculated by eq 1. [b] Average number of monomers evaluated from eq 2. [c] Average molecular weight calculated from eq 3 with $MW_{MonomerP1} = 175$ and $MW_{MonomerP2} = 116$; see Experimental Section. [d] Average distance between individual polymer molecules that is obtained by converting 2 mg mL^{-1} by (i) taking into account the experimentally evaluated average molecular weight $\langle MW \rangle$; (ii) assuming the polymer molecules to be distributed over a cubic lattice: $\langle r \rangle$ (nm) $\approx 0.1/(N_A C)^{1/3}$, where N_A designates the Avogadro number and C the molar concentration of the polymer (for details, see Experimental Section).

average molar masses. It is possible to evaluate a hydrodynamic radius for the polymers considered as random coils in a good solvent, and to convert the corresponding characteristic radii into polymer lengths or conversely to an average molar mass from the appropriate scaling law (see Experimental Section). Table 1 lists the results. The radii R(**P**) calculated according to eq 1 are in the range of 2−6 nm. This is large enough to obtain sufficiently thick polymer monolayers for covering the gold surfaces. Yet the layers remain thinner than the $\lambda/2$ maximum probing range of the techniques used to detect adsorption on gold.

Functionalization of Gold Surfaces by Polymer Monolayers. First, the interaction between the hydrophilic polymers and citrate-capped gold nanospheres (diameter 12 nm; see Experimental Section) was investigated. UV/vis absorption spectra from dispersions of the gold colloids were recorded after 12 h of incubation with increasing amounts of polymers. Figure 2a and b displays typical results for the polymer **P1S** containing disulfide anchoring groups. With increasing concentration, the plasmon resonance absorption is enhanced and red-shifted (Figure 2a). Beyond concentrations of about 0.05 mg mL^{-1}, a plateau is reached; the absorbance is increased by about 10%, and the absorption maximum shifts from 519 nm (initial dispersion of gold colloids) to 523 nm at saturation (Figure 2b). The observed red shift of the plasmon resonance frequency is too small to be attributed to particle aggregation (vide infra). Yet the observed shift is in line with a rise of the dielectric

(18) Heinz, B. S.; Laschewsky, A.; Rekaï, E. D.; Wischerhoff, E.; Zacher, T. In *Stimuli-Responsive Water-Soluble and Amphiphilic Polymers*; McCormick, C. L., Ed.; ACS Symposium Series 780; American Chemical Society: Washington, DC, 2001; Chapter 10, pp 162−180.

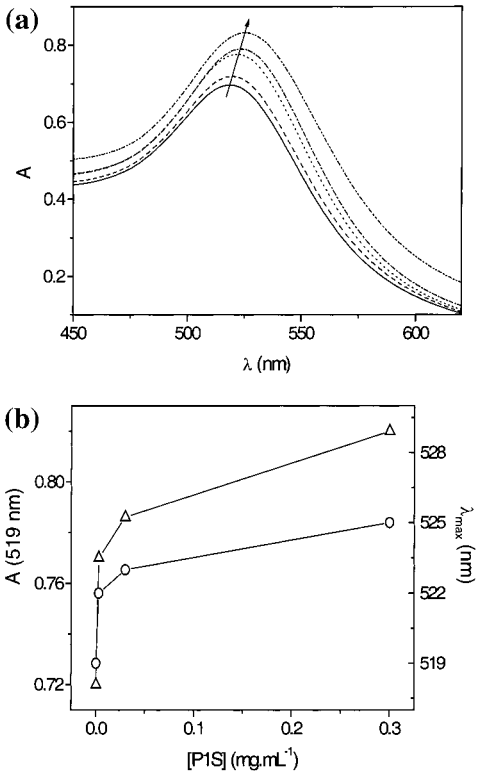

Figure 2. (a) Influence of **P1S** concentration on the UV/vis absorption spectrum of a 4 nM aqueous solution of gold colloids. **P1S** concentration (mg mL^{-1}), from bottom to top: 0 (solid line), 0.0003 (dashed line), 0.003 (dotted line), 0.03 (long dashed−dotted line), 0.3 (dashed−double dotted line). (b) Absorbance at 519 nm (△) and wavelength λ_{max} at absorption maximum (○) as a function of **P1S** concentration.

constant of the medium surrounding the gold colloids according to the Mie theory.[2] Similar results were obtained for the other polymers bearing disulfide groups, **P1nS** and **P2S**. Thus, UV/vis absorption spectra provide evidence that the disulfide-bearing polymers and the gold colloids interact without causing colloid aggregation. Noteworthy, some changes of the colloid spectral properties, albeit smaller, were also observed when applying the reference polymers **P1I** and **P2I** that do not bear disulfide functions.

To evaluate more quantitatively the significance of the disulfide group for the anchoring of the polymers, absorbance data A_λ([**P**]) were used to extract an order of magnitude of the affinity constants K(**P**) of the polymers **P** for the gold colloids (see Experimental Section). Table 2 summarizes the results of analyzing the absorbances at 519 nm. The affinity constants of **P1S** and of **P1nS** for the gold surface are respectively 4 and 2 times larger than that of **P1I**, whereas the corresponding constants for **P2S** are twice larger than that of **P2I**.

The order of magnitude of the thickness h_1(**P**) of polymer coatings on gold colloids was derived from dynamic light scattering. Table 2 sums up the results. The hydrodynamic diameter of the bare gold colloids was found equal to 15 nm. This value satisfactorily compares with the 12 nm diameter extracted from electron microscopy if one considers the citrate ions capping the colloids so as the water primary solvation shell. The normalized ratios h_1(**P**)/R(**P**) are significantly lower for the **PI** polymers than those in the **PS** series.

SPR measurements of the polymers grafted on planar gold surfaces provide complementary insights to those obtained on

Table 2. Modification of Gold Surfaces by Polymers **P1I**, **P2I**, **P1S**, **P2S**, and **P1nS**: Affinity Constants K of the Polymers for Gold Colloids at 295 K As Extracted from UV/Vis Spectra, Hydrodynamic Diameter D, and Corresponding Polymer Thickness h_1 of Polymer-Coated Gold Colloids As Measured by Dynamic Light Scattering, SPR Asymptotic Shifts $\delta I(\infty)$ at Infinite Polymer Concentration and Corresponding Thicknesses h_2 of the Polymer Layer (cf. Text and Experimental Section)

polymer **P**	$K \pm 20\%$[b]	$D \pm 20\%$ (nm)[c]	$h_1 \pm 20\%$ (nm)[d]	$\delta I(\infty)$ (mV)	$h_2 \pm 20\%$ (nm)	h_1/R[a]	h_2/R[a]
P1I	4.9×10^5	34	11	0.09	1.1	1.8	0.2
P2I	1.2×10^5	16	2	0.02	0.4	0.9	0.2
P1S	1.8×10^6	29	8.5	0.18	3.0	2.7	0.9
P2S	2.6×10^5	29	8.5	0.22	4.4	3.1	1.6
P1nS	9.3×10^5	54	21	0.17	2.8	8.1	1.1

[a] h_1/R and h_1/R are calculated for comparison using data given in Table 1. [b] See eq 5; standard state: ideal solute at 1 M for the infinitely diluted solution. [c] Derived from eq 1. The hydrodynamic diameter of bare gold colloids was found equal to 15 nm. [d] Equal to $0.5(D - 12)$, where 12 nm designates the diameter of the bare gold colloid as measured by electron microscopy.

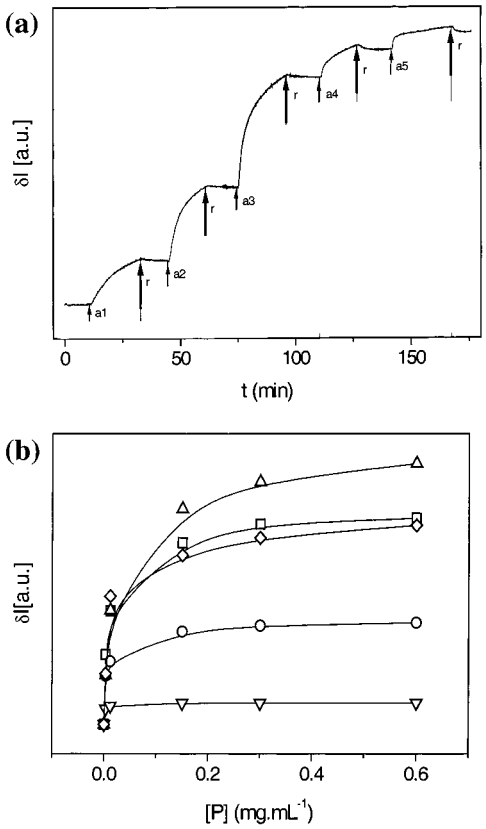

Figure 3. (a) Evolution of the SPR intensity at a fixed angle at various concentrations of **P2S**. Several consecutive steps can be distinguished. Thin arrows: additions of **P2S** (a1, 0.003 mg mL^{-1}; a2, 0.012 mg mL^{-1}; a3, 0.15 mg mL^{-1}; a4, 0.3 mg mL^{-1}; a5, 0.6 mg mL^{-1}). Thick arrows: rinsing with buffer (r). (b) Influence of polymer concentrations [**P**] on the SPR intensity at the fixed angle. **P1S** (□), **P2S** (△), **P1nS** (◇), **P1I** (○), **P2I** (▽).

gold colloids. The introduction of the polymers bearing disulfide groups in the SPR cell induces strong shifts of the SPR signal. In the case of **P2S**, the evolution of the differential signal δI as a function of time indicates that the grafting occurs within about 10 min, and is concentration-dependent (Figure 3a). As for the gold colloids (cf. Figure 2b), a plateau is observed at the largest concentrations of **P2S** (Figure 3b). Once again, this is interpreted in terms of the formation of a polymer monolayer. Comparable results were observed for all the polymers investigated. Figure

3b shows that most of the curvature of the $\delta I([\mathbf{P}])$ curves lies in the same range of 0.05 mg mL^{-1} for all the polymers. This observation is in line with the rather similar affinity constants that were derived from the UV/vis experiments on the gold colloids (see Table 2). Table 2 summarizes the limit $\delta I(\infty)$ values that were obtained at the plateau with the polymers investigated, and the thicknesses h_2 of the polymer layers. They were derived from $\delta I(\infty)$ using the standard Fresnel equations and appropriate orders of magnitude of the different refractive indexes for the polymer layers assumed to contain no water (see Experimental Section). As for gold colloids, the normalized thicknesses $h_2(\mathbf{P})/R(\mathbf{P})$ of the polymer layers on planar surfaces are significantly larger in the **PS** series than those in the **PI** series. However, the $h_2(\mathbf{P})$ values are significantly smaller than the corresponding values $h_1(\mathbf{P})$ found on gold colloids. Although surface curvature makes quantitative comparisons difficult, the difference probably reflects the presence of a significant amount of water within the polymer layer.

Surprisingly, the disulfide-bearing polymers exhibit only a slightly larger affinity for the gold surfaces than those that do not dispose of disulfide groups. The observation is discussed in relation with the sources of polymer−gold interaction. In addition to the specific sulfur−gold bond, another attractive component is expected from an unspecific polymer−gold interaction originating from hydrophobic forces.[19] Its significance depends on the contact surface between gold and the polymer. For a given polymer average molar mass, the contact surface will depend on polymer conformation; much stronger energies of interaction are anticipated when the polymer lies flat on surfaces. In the present case, indirect information about the polymer conformation in the coating monolayer is provided by the evaluation of the normalized thickness $h_i(\mathbf{P})/R(\mathbf{P})$ of the monolayers. Table 2 shows that the normalized thicknesses of monolayers made from **PI** are always lower than those made from **PS**. These observations suggest that **PI** polymers probably adopt flatter conformations on gold surfaces than do **PS** polymers. Under such conditions, one anticipates the significance of the energetic contribution of unspecific adsorption to the polymer affinity for gold to be larger in the **PI** series than in the **PS** series. The relative importance of the disulfide group for binding would probably then exceed the factors 2−4 derived from the determinations of the affinity constants. In fact, the sulfur−gold bond is strong enough to overcome the unfavorable entropic contribution resulting from the conformational change of the polymer backbone that is required to expose the polymer disulfide moiety for the anchoring onto gold. **P1nS** deserves a special comment. Despite the anticipated larger number of disulfide anchor groups along the polymer backbone, **P1nS** does not exhibit a much larger affinity for gold than does **P1S**. This could be explained by (i) an unfavorable enthalpy−entropy balance if multiple anchoring induces a too large contraction of the conformational space, (ii) the lower molar mass of **P1nS**, or (iii) by a different polymer topology (star/graft vs linear). The localization of the disufide group in **P1nS** may be less favorable for the anchoring on gold than in **P1S**. In fact, the steric hindrance for the forming of a gold−disulfide bond might be higher if the anchor is located along the polymer chain instead of at its extremity.

Stability of Polymer Anchoring on Gold Surfaces. Dense monolayers obtained by self-assembly of low molecular weight thiols on gold are stable in aqueous solution. Nevertheless, we were concerned with the stability of corresponding layers made from hydrophilic disulfide-bearing polymers **PS** which seemed to be only slightly larger than those of the reference polymers **PI**. Therefore, we investigated a possible release of the grafted polymers upon washing or dilution. Figure 3a shows that almost no **P2S** polymer is removed from the gold surface when rinsing the grafted surface below the plateau shown in Figure 3b. Thus, the docking of **P2S** on gold remains strongly favored below saturation. In contrast, one observes a small desorption of polymer at the largest concentrations investigated. This is probably a result of the much lower affinity of the polymer toward the already derivatized gold surface. It is also possible that the characteristic time to disentangle the compact polymer monolayer is larger than that of a less compact layer. Similar observations were made with the other disulfide-bearing polymers. We also tested the stability of the anchored polymers on gold under more stringent conditions by washing the layer with 1:1 methanol:HCl 37%. This cleaning method effectively removes organic compounds from glass slides[20] without altering the gold surface as we have checked by SPR. After the washing step, 15% of the **P2S**, 60% of the **P1S**, and 60% of the **P1nS** polymer layers remained on the gold surface; the latter result is rather satisfactory and underlines the stability of the **P1S** and **P1nS** polymer-coated surface. Investigations with the gold colloids confirmed the SPR results. In fact, it was possible to purify gold colloids grafted with disulfide-bearing polymers by gel permeation chromatography (vide infra). In this case, the polymer in excess remaining in the aqueous solution after saturation of the gold surface is removed. Nevertheless, the removal never changed the UV/vis absorption spectrum of the colloids nor their stability to precipitation upon addition of NaCl (vide infra). These observations confirm that the affinity of the disulfide-containing polymers toward gold surfaces and/or the kinetic inertness of derivatized metal nanoparticles were high enough to resist washing and dilution under most experimental conditions. However, it will be shown below that large amounts of low molecular weight thiol-containing compounds may displace the disulfide-bearing polymers from the gold surface.

Investigations of the Features of the Polymer Monolayers on Gold. Two different issues were addressed. We were first concerned with the steric protection of the gold surface by the polymer monolayers, which are expected to reduce unspecific adsorption on the metal surface. In addition, we wanted to evaluate whether the protection was not detrimental to the free diffusion of different types of solutes within the polymer monolayer. These features are important for potential biological applications.

Gold colloids strongly tend to adsorption or aggregation due to the large attractive term at short range originating from the

(19) The interaction potential between two citrate-stabilized gold colloids is expected to exhibit a barrier separating two minimas located respectively at very short and long distances. The minima originate from the balance between the strong short-range attractive van der Waals dispersive interaction and the long-range repulsive electrostatic interaction. The adsorption of a polymer generates an additional repulsive energy term arising from the steric repulsion between polymer monolayers. This will change the location and the depth of the two energy minima, so as the height of the energy barrier. Consequently, both the thermodynamics and the kinetics of aggregation will be modified. See, for instance: Israelachvili, J. N. *Intermolecular and Surface Forces*, 2nd ed.; Academic Press: London, San Diego, New York, Boston, Sydney, Tokyo, Toronto, 1992.

(20) Cras, J. J.; Rowe-Taitt, C. A.; Nivens, D. A.; Ligler, F. S. *Biosens. Bioelectron.* **1999**, *14*, 683−688.

dispersive van der Waals interaction in aqueous solutions.[19] For instance, the direct exchange of the external medium resulting from the citrate reduction of Au(III) salts could not be done by gel permeation chromatography as the gold particles precipitated on the top of the column. Similarly, instantaneous colloid aggregation was observed upon addition of various additives (salts, organic molecules, ...) to the suspensions. The derivatization of the gold surface by the disulfide-bearing polymers considerably improved the colloid stability toward aggregation. The gold colloids remained water-soluble during the derivatization process, and filtration, centrifugation, and gel permeation chromatography could be applied to polymer-grafted particles. Furthermore, these polymer-modified gold colloids can be lyophilized and then redispersed in water. This behavior is usually considered to indicate the complete protection of gold colloids by the polymer monolayer. The excellent dispersion of the modified colloids in aqueous media is an important result by itself since relatively few water-soluble, modified-gold colloids have been reported yet.[21] Even less systems have been described that yield uncharged water-soluble gold nanoparticles.[22]

To obtain a more quantitative picture about the steric protection, we applied an aggregation test to the different gold colloids−polymer mixtures. The latter consists of adding aliquots of 5 M aqueous NaCl to colloidal solutions while following any salt-induced aggregation by UV/vis absorption spectroscopy. Without protection by a polymer monolayer, the gold particles rapidly precipitated when exposed to aliquots of 5 M aqueous NaCl. When protected by polymer monolayers, two different behaviors were typically observed as displayed in Figure 4a for the series **P1**. For colloidal solutions containing **P1I**, the addition of salt induces (i) a decrease of the plasmon resonance band and its shift from 523 to 536 nm, and (ii) a pronounced shoulder at the lower wavelength side. These changes of the UV/vis absorption spectrum are attributed to an aggregation of the gold particles. In contrast, only slight changes were observed after the addition of NaCl in the spectrum for gold colloids coated with **P1S**. Figure 4b displays the ratio of the intensities of the plasmon resonance band, before and after the addition of NaCl, as a function of **P1S** concentration. As already seen in Figure 2b, a plateau manifests itself beyond 0.05 mg mL^{-1}. Table 3 summarizes the efficiency of the different polymers against NaCl-induced aggregation. Although exhibiting similar affinities for gold, the polymers bearing disulfide groups are clearly much better stabilizers than are the reference polymers without special anchor groups.

The precise role of the disulfide moiety in the stabilization of gold colloids against aggregation is first addressed in relation with the DLVO theory.[19] The thermodynamic issue is first discussed. The structures of the backbone of **PI** and **PS** are similar. In contrast, the analyses of dynamic light scattering and SPR data suggest that the monolayers should be thicker in the **PS** series than in the **PI** series. Under such conditions, the energy minimum at short distances should be deeper in the **PI** series (shorter distance = stronger van der Waals attraction) than in the **PS** series. This should disfavor salt-induced aggregation of

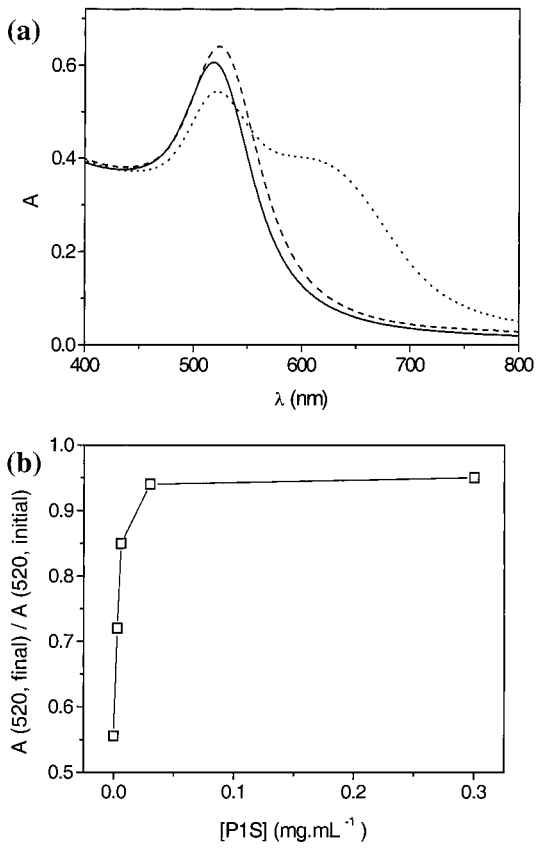

Figure 4. (a) Absorption spectra of 3.5 nM Au colloids: naked (solid line), after NaCl addition in the presence of 0.026 mg mL^{-1} of **P1S** (dashed line), after NaCl addition in the presence of 0.026 mg mL^{-1} of **P1I** (dotted line). (b) Influence of the concentration of **P1S** on the intensity of the band at 520 nm after exposure to NaCl. The intensity is normalized to the signal intensity before NaCl addition. The concentration [**P1S**] refers to that before dilution by addition of aqueous NaCl. See Experimental Section.

Table 3. NaCl-Induced Aggregation Tests on Gold Colloids at 295 K, as a Function of the Concentration of the Monolayer Forming Polymers **P1I**, **P2I**, **P1S**, **P2S**, and **P1nS**[a]

[**P**] (mg mL^{-1})	P1I	P2I	P1S	P2S	P1nS
3×10^{-4}	+	+	+	+	+
3×10^{-3}	+	+	+	+	+
3×10^{-2}	+	+	−	−	−
3×10^{-1}	+	+	−	−	−

[a] The symbols "+" indicate the presence and the symbols "−" indicate the absence of aggregation, as followed by UV/vis absorption.

the **PS** series in the thermodynamic regime. The same reasoning applies for the kinetics of aggregation. **PS**-coated gold colloids are kinetically better protected against aggregation than are the **PI**-coated colloids due to the stronger steric stabilization. Other factors in relation with the affinity of the polymers for gold are also relevant for discussing the significance of the disulfide moiety. First, the extent of formation of the polymer monolayer at a given concentration will be larger in the **PS** series than in the **PI** series since the corresponding affinity for the gold surface is larger in the former series (vide supra). Consequently, the aggregated state will be less favored in the **PS** series than in the **PI** series at comparable concentrations. One eventually addresses the kinetics of the undocking process of the polymer from the surface of the gold colloids. Whereas the affinity constants are rather similar in both series **PI** and **PS**, nothing is known a priori about the relative values of the kinetic constants

(21) (a) Templeton, A. C.; Cliffel, D. E.; Murray, R. W. *J. Am. Chem. Soc.* **1999**, *121*, 7081−7089. (b) Templeton, A. C.; Chen, S.; Gross, S. M.; Murray, R. W. *Langmuir* **1999**, *15*, 66−76.
(22) (a) Bartz, M.; Küther, J.; Nelles, G.; Weber, N.; Seshadri, R.; Tremel, W. *J. Mater. Chem.* **1999**, *9*, 1121−1125. (b) Liu, J.; Ong, W.; Roman, E.; Lynn, M. J.; Kaifer, A. E. *Langmuir* **2000**, *16*, 3000−3002.

Table 4. SPR Investigations of the Adsorption of 0.5 g L^{-1} of BSA and Human Serum onto Polymer-Coated Gold Surfaces

surface	δI due to BSA (mV)	δI due to human serum (mV)	total δI (mV)
bare gold	0.063	0.015	0.078
P1I-coated gold	0.026	0.038	0.064
P2I-coated gold	0.016	0.085	0.101
P1S-coated gold	0.003	0.003	0.006
P2S-coated gold	−0.025	−0.005	−0.030
P1nS-coated gold	0.023	0.035	0.058

associated to the docking and undocking processes. In fact, the docking is expected to occur faster in the **PI** series. Indeed, the unspecific binding involving surface−surface interactions of the former series is much less constraining than the specific site−surface interaction of the latter. Consequently, undocking is expected to take place much faster in the **PI** series. This picture is supported by SPR experiments and gel permeation chromatographic studies for which kinetic inertness was evoked to account for the results. This feature should also contribute to slow the aggregation of gold colloids if partial removal of polymers from the monolayer coating on colloids is required at thermodynamic equilibrium. In agreement with the preceding points, the experimental behavior of the disulfide-containing polymer toward aggregation was singular as compared to that of the reference polymers. No aggregation was observed in the **PS** series above certain concentrations of polymers at the experimental time scale. Unfortunately, one cannot easily determine which factor evoked above dominates the behavior since we do not know whether the final observed state is a true state of equilibrium, or whether the relaxation of the system was not complete at the end of our experiments.

In a second series of experiments, we were concerned with the possible unspecific adsorption of BSA/human serum on the hydrogel surface coatings. The results of the corresponding SPR experiments are displayed in Table 4. The increase in SPR intensity on adsorption of BSA onto the bare gold surface indicates that BSA strongly adsorbed to form a monolayer on the surface.[23] The additional increase on interaction of the surface with human serum shows that the surface was eventually blocked with a monolayer of proteins. The behavior observed in the presence of **P1I** and **P2I** is rather similar and is in line with the large kinetic lability of the corresponding polymer monolayers that was evoked to account for the aggregation results. In contrast, adsorption of BSA and human serum onto a gold surface coated with the polymer **P1S** was considerably reduced. Hence, the increase due to BSA was only 4% of that onto the bare Au surface, and the total unspecific binding of protein was reduced to 6%. The present results compare well with those obtained with PEG-coated gold surfaces where unspecific adsorption of serum proteins was shown to be suppressed down to by 4.2−6.25% of the original value.[24] The behavior of **P2S**-coated gold surfaces was rather surprising. In fact, the SPR signal decreased unexpectedly during the studies on the unspecific adsorption of BSA and human serum. Two explanations could account for the latter observation. First, the decrease could be due to a displacement of polymer **P2S** by competitive adsorption of proteins. The larger affinity of the **P1S** polymer toward gold would preclude such a displacement in the experiments with **P1S**. Second, one could also envisage that BSA adsorption induces some conformational rearrangement in the polymer monolayer of **P2S** leading to the observed decrease of the SPR signal. Eventually, **P1nS** again exhibits a marginal behavior which probably reveals that the surface of gold is only partially passivated against unspecific adsorption.

Table 5. Kinetic Constants k Derived from Etching Experiments with Gold Colloids Coated with Polymers **P1I**, **P2I**, **P1S**, **P2S**, and **P1nS** at 295 K (k Is Derived from the Initial Slopes of the Curves $\ln[A(520,t)/A(520,0)]$ as a Function of Time, See Experimental Section)

polymer	k (min^{-1})
none	2.3
P1I	1.4
P2I	0.7
P1S	0.09
P2S	0.06
P1nS	1.0

Also, we addressed the issue of permeability of the disulfide-bearing polymer monolayers grafted on gold to low molar mass species, and their diffusion within the gels. We examined the kinetics of the loss of the plasmon resonance band of gold resulting from the reaction with etchant species which converts Au(0) to $[Au(CN)_4]^-$.[25] The rate of the dissolution of the gold particles is related to the efficiency by which a particular polymer provides a protective barrier against small species. Figure 2S shows that the drop of the plasmon resonance absorption associated to the dissolution of gold follows a first-order kinetics, as observed in all cases. Table 5 summarizes the kinetic constants derived from these measurements. In the case of uncoated gold colloids, the plasmon band of the gold particles disappears nearly in less than 30 s. In the case of the polymers **P1I** and **P2I**, the protection against dissolution is poor. Such a result is anticipated if the polymer monolayers are loose or thin as suggested by dynamic light scattering and SPR experiments. In contrast, the dissolution of the gold colloids coated with disulfide-bearing polymers is much slower, except for **P1nS**. The particular behavior of the latter polymer may result from its different architecture that does not bring a significant advantage; recall that the affinity of **P1nS** to gold was not improved over other disulfide-bearing polymers and that large unspecific adsorptions were observed on **P1nS**-coated gold surfaces (vide supra). In fact, increased conformational constraints would probably reduce the local density of polymer chains close to the gold surface so as to facilitate access of the etching agents to the gold surface. In contrast, the results obtained for **P1S** and **P2S** indicate the formation of an efficient barrier against small chemical agents that does not forbid their diffusion within the polymer monolayer. Because etching is not totally inhibited, one cannot exclude the presence of unprotected surface areas that could lead to some unspecific adsorption of fragile materials such as biomolecules. To remedy this potential problem, we envisaged to complete the coverage of the gold surface with hydrophilic thiols of low molecular weight, such as 3-mercapto-1,2 propane diol (MPDiol), which could diffuse

(23) BSA has an ellipsoidal structure with dimensions of 11.6 × 2.7 × 2.7 nm^3. See: Riddiford, C. L.; Jennings, B. R. *Biochim. Biophys. Acta* **1966**, *126*, 171−173.

(24) Kenausis, G. L.; Vörös, J.; Elbert, D. L.; Huang, N.; Hofer, R.; Ruiz-Taylor, L.; Textor, M.; Hubbell, J. A.; Spencer, N. D. *J. Phys. Chem. B* **2000**, *104*, 3298−3309.

(25) (a) Chen, S. *Langmuir* **1999**, *15*, 7551−7557. (b) Templeton, A. C.; Hostetler, M. J.; Kraft, C. T.; Murray, R. W. *J. Am. Chem. Soc.* **1998**, *120*, 1906−1911. (c) Marinakos, S. M.; Novak, J. P.; Brousseau, L. C., III; Blaine House, A. B.; Edeki, E. M.; Feldhaus, J. C.; Feldheim, D. L. *J. Am. Chem. Soc.* **1999**, *121*, 8518−8522.

through the polymer layer. Thus, the effect of the addition of MPDiol to aqueous suspensions of the different polymer-coated gold colloids was analyzed by means of the preceding etching test as well as of the aggregation test. In all cases, the gold colloids dissolve much more slowly than in the case of the polymer-modified colloid in the absence of MPDiol (Figure 2S). Hence, a very efficient barrier against etching agents is formed. However, the addition of less than 0.3 mL of 5 M NaCl led to the instantaneous aggregation of the particles of all the samples. Because under the same conditions, no aggregation was observed for the polymer-coated colloids (see Table 3), these findings suggest that MPDiol does efficiently graft on the gold surface while displacing the polymer chains already anchored. Eventually, the MPDiol monolayer formed is no longer able to provide good colloidal stability.

Behavior of Gold Colloids Coated with Thermoresponsive Polymers. The preceding experiments demonstrated that the grafting of large molecules on gold surfaces induced only rather small perturbations of the properties of the gold colloids. This is desirable for a protection of the colloids. But for biosensor applications, this implies that the signals obtained for such systems from UV/vis absorption spectra of the plasmon resonance band, or from SPR, are not very sensitive to the selective binding of analytes. Therefore, we explored whether such perturbations could be enhanced by taking advantage of the thermal collapse of polymers derived from monomer **2** at the lower critical solution temperature. Such a phenomenon should strongly modify the refractive index of the layer covering the gold surface, and consequently enhance the signal response. Hence, the evolution of the absorption spectrum of **P2S**-derivatized gold colloids was investigated as a function of temperature. For comparison, the same experiment was performed on naked gold particles as well as on **P1S**-modified gold colloids that do not exhibit a thermal transition. In the latter cases, no change of the plasmon band was observed upon heating, except for a small decrease of its intensity which is attributed to solution dilatation. In contrast, a marked red shift of the plasmon band from 523 to 537 nm and a strong increase of the band intensity were observed for **P2S**-derivatized gold colloids when raising the temperature from 300 to 315 K (Figure 5a). Figure 5b displays the changes of the plasmon band intensity recorded at 520 nm of an aqueous suspension of **P2S**-modified gold colloids as a function of temperature. The latter curves show a transition around 308 K. This transition temperature compares well with the LCST measured for **P2S** in aqueous solution.[26] In contrast, the breadth of the transition is much sharper for **P2S**-coated gold colloids than for **P2S** in aqueous solution. The latter behavior probably results from the grafting on colloids/gel permeation chromatography process. In fact, molecules exhibiting the largest affinity for the gold surface in the **P2S** sample preferentially adsorb on metal. By considering that the corresponding affinity depends on polymer length (vide supra) and that unadsorbed **P2S** molecules are discarded during the subsequent chromatographic separation, one thus expects a decrease of polydispersity manifesting itself as a sharper thermal transition. In addition, a similar although more pronounced

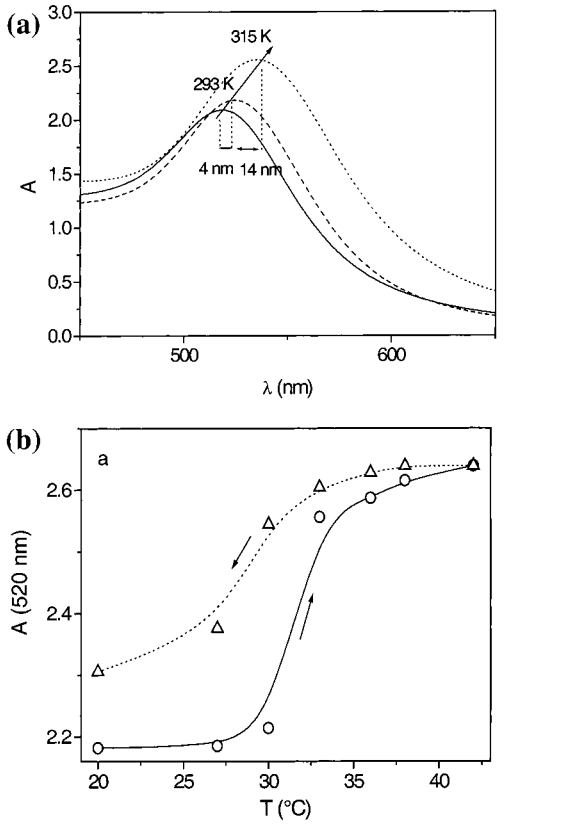

Figure 5. (a) UV/vis spectral changes occurring during the temperature increase of an aqueous suspension of **P2S**-modified gold colloids (12 nM). Solid line, naked gold colloids at 293 K; dashed line, **P2S**-coated gold colloids at 293 K; dotted line, **P2S**-coated gold colloids at 315 K. (b) Changes of the plasmon band intensity at 520 nm of an aqueous suspension of **P2S**-modified gold colloids (12 nM) as a function of temperature.

hysteresis as displayed in Figure 4S was observed during the cooling cycle. Such a behavior is in line with the much larger size of the **P2S**-coated gold colloids. Correspondingly, the rate of the desaggregation process decreases during the cooling step.

To support that the thermoresponsive behavior of the **P2S**-derivatized gold colloids was linked to the temperature-induced conformational change of the polymer, a series of samples was studied by transmission electron microscopy (TEM). A drop of the solution of gold colloids stabilized with poly(*N*-vinylpyrrolidone) was evaporated slowly onto a carbon-coated copper mesh grid, and the resulting structures were examined. Bright field TEM micrographs of the stabilized nanoparticles revealed well-dispersed particles with an average diameter of 12 nm and of narrow size distribution (±1 nm). Figure 6a and b displays the corresponding pictures obtained with aqueous dispersion of gold particles derivatized by **P2S** after evaporation at 298 K, and at 333 K, that is, below and above the thermal transition in solution. The comparison of these two pictures shows that the average distance between Au nanospheres is much smaller at 333 K than at 298 K. This finding is in line with (i) a conformational collapse of the sterically protective polymer monolayer grafted on the surface of the gold particles occurring in the [298 K; 333 K] range; the collapse is known to be associated to an increase of hydrophobicity at the largest temperatures; and (ii) a temperature-induced aggregation of the gold particles resulting from hydrophobic interactions between **P2S**-coated gold colloids.

(26) A cloud point of 306 K was determined for **P2S** from the inflection point of the curve obtained during the heating cycle (Figure 4S). Though this value is in line with previous reports on **poly-2** in aqueous solutions at similar concentrations, the broad thermal transition observed for **P2S** differs from many reports (see ref 17). The broadness of the transition presumably originates from the large polydispersity of sample **P2S**.

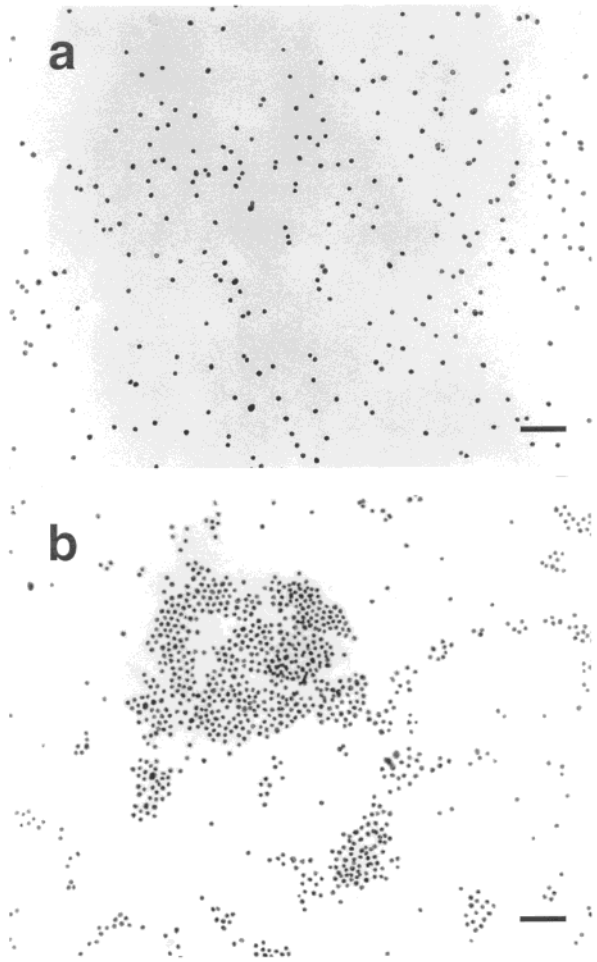

Figure 6. TEM images of gold colloids. (a) **P2S**-coated particles evaporated at room temperature. (b) **P2S**-coated particles evaporated at 333 K. The bar displays 100 nm.

Significant temperature-induced modifications of the optical properties of gold nanoparticles have been reported before.[27] The temperature-dependent assembly of complementary single-strand oligonucleotides was used to tune the average interparticle distance and to eventually control the electronic coupling between gold colloids.[28] In the present system, the average molar mass of **P2S** still gives too thick polymer layers to allow the observation of the change of the coupling regime above the cloud point. In principle, one could prepare smaller **P2S** molecules. Thus, one may envisage to intensify the optical response to interaction with the substrate to be analyzed by playing not only with the change of the refractive index above the cloud point, but also by using the polymer collapse-induced aggregation of the gold nanoparticles. The latter phenomenon could also find some applications for reversibly tuning the optical features of gold sols,[29] or for the electronic properties of quantum dot solids when using smaller metal particles.[30]

All findings support that (i) a temperature-induced conformational collapse of **PS2** does occur on gold colloids; and (ii) the change of the UV/vis signal induced by the polymer collapse is larger than the corresponding one accompanying the simple adsorption of a large molecule (such as the hydrophilic polymers) on the gold surface. Considering SPR observations made with other polymers exhibiting a LCST,[31] the present results confirm that a thermal transition can be reasonably considered as a means to enhance the signal response for detecting adsorption on gold surfaces, by methods such as UV/vis absorption, or by SPR.

Conclusion

The surface of gold colloids can be easily and efficiently derivatized in aqueous solution with hydrophilic nonionic polymers that bear terminal disulfide anchoring groups. The resulting polymer-coated gold nanoparticles can be stored in the dry state and redispersed in water, to yield sterically stabilized colloid suspensions. The polymer layers allow free diffusion of small solutes, but minimize efficiently the unspecific absorption of large molecules such as proteins. Such features are most attractive for biological applications, especially upon taking into account the versatility of the polymer approach for surface derivatization. In fact, it is easy to change the average molecular mass of the polymers, to introduce diverse functionalities such as reactive groups along the polymer backbone, and so on. Further, the study underlines the possible advantage to introduce components making the hydrogel surface coatings an "active" partner in a sensing purpose. For example, our investigations suggest that a suitably tuned phase transition could amplify the response toward external stimuli when using optical methods for the detection, like UV/vis absorption for gold colloids, or SPR for gold surfaces.

Experimental Section

Materials. Hydrogen tetrachloroaurate (Aldrich), sodium citrate (Aldrich), sodium chloride (Acros), potassium cyanide (Acros), and potassium ferricyanide (Prolabo) were used without further purification. Doubly distilled water was purified by a Millipore system.

Polymer Synthesis. The synthesis of the disulfide-functionalized initiators was reported previously.[13,16] The synthesis of polymers **P1S** and **P2S** with a disulfide-functionalized initiator is described elsewhere.[18] Reference polymers **P1I** and **P2I** were obtained by the analogous procedures employing the initiator azoisobutyronitrile (AIBN). Polymer **P1nS** was made by polymerizing monomer **1** with the photoinitiating system of oligo(oxy-1,2-dithiane 4,5-diyl-oxycarbonyliminohexamethylene imino carbonyl)-*co*-(oxy dimethylene *N*-phenyliminodimethylene-oxycarbonyl iminohexamethylene iminocarbonyl) **nS**/2-(2′-hydroxy-3′-trimethylammoniopropyloxy)thioxanthone chloride, in analogy to ref 13.

Evaluation of Hydrodynamic Radii from NMR Experiments. The measurements of translational diffusion coefficients at 300 K were carried out on an Avance Bruker DRX 600 spectrometer equipped with a TBI probe with three orthogonal pulsed field gradients (PFG). The pulse sequence used is a stimulated echo (STE) with residual solvent signal suppression.[32] Eddy current effects were minimized using sine shaped PFG and introducing a longitudinal eddy current delay (LED) of 5 ms before acquisition. The diffusion delay length (Δ) was 600 ms, and encoding PFG lengths (δ) were of 2 ms for all experiments, except for the sample **P1I** ($\Delta = 1$ s and $\delta = 3$ ms). Their maximum amplitudes were varied from 5.5 to 52.9 G cm^{-1} in 32 steps. Each was acquired with 256 transients. Suppression of HOD signal was achieved

(27) Mirkin, C. A. *Inorg. Chem.* **2000**, *39*, 2258−2272.
(28) Lazarides, A. A.; Schatz, G. C. *J. Phys. Chem. B* **2000**, *104*, 460−467.
(29) Xia, Y.; Gates, B.; Yin, Y.; Lu, Y. *Adv. Mater.* **2000**, *12*, 693−713.
(30) (a) Markovich, G.; Collier, C. P.; Heinrichs, S. E.; Remacle, F.; Levine, R. D.; Heath, J. R. *Acc. Chem. Res.* **1999**, *32*, 415−423. (b) Martin, J. E.; Wilcoxon, J. P.; Odinek, J.; Provencio, P. *J. Phys. Chem. B* **2000**, *104*, 9475−9486.
(31) Wischerhoff, E.; Zacher, T.; Laschewsky, A.; Rekaï, E. D. *Angew. Chem., Int. Ed.* **2001**, *39*, 4602−4604.
(32) Altieri, A. S.; Hinton, D. P.; Byrd, R. A. *J. Am. Chem. Soc.* **1995**, *117*, 7566−7567.

using two 270° Gaussian pulses of 2 ms. Diffusion coefficients were obtained by fitting the decrease of the signals with respect to gradient intensity. The average values correspond to peaks with good enough signal-to-noise ratios.

Data Analysis. An average hydrodynamic radius R of each polymer sample was derived from the measured self-diffusion coefficient D_t according to the Stokes−Einstein relation:

$$D_t = \frac{kT}{6\pi\eta R} \quad (1)$$

for a random coil where η designates the solvent viscosity, T the absolute temperature, and k the Boltzmann constant. The hydrodynamic and gyration radii were then assimilated to eventually derive an order of magnitude of an average number N of monomers contained within the polymer according to:[33]

$$N \approx \left[\frac{kT}{6\pi\eta a D_t}\right]^{5/3} \quad (2)$$

where a designates the monomer length evaluated to 0.25 nm in the present series of polyacrylamides from Hyperchem molecular modeling. Eventually, an estimate of an average molecular weight[34] of each polymer sample ⟨MW⟩ was obtained from:

$$\langle \mathrm{MW} \rangle \approx \left[\frac{kT}{6\pi\eta a D_t}\right]^{5/3} \times \mathrm{MW}_{\mathrm{monomer}} \quad (3)$$

where $\mathrm{MW}_{\mathrm{monomer}}$ designates the molecular weight of the monomer that was used for the polymer synthesis.

It was checked a posteriori that NMR experiments were performed in the dilute regime to reasonably interpret the radii $R(\mathbf{P})$ as characterizing the polymer random coils. Taking into account the extracted radii $R(\mathbf{P})$, it is possible to evaluate the order of magnitude of the average molar mass of each polymer sample from eqs 2 and 3. In fact, assuming that the macromolecules are distributed on a cubic lattice, it was always found that the average distance $\langle r(\mathbf{P}) \rangle$ between polymer coils remained less than $0.2R(\mathbf{P})$ at the polymer concentrations used (2 mg mL^{-1}) (Table 1).

UV/Vis Absorption Experiments. UV/vis absorption spectra were recorded on a Kontron Uvikon-930 spectrophotometer. The temperature was regulated at 0.1 °C and directly measured within the 1 cm × 1 cm cuvette. Cloud point experiments were performed by recording the absorbance at 260 nm as a function of temperature on aqueous solutions containing either 0.36 mg mL^{-1} of polymer **PS2** or 12 nM **PS2**-derivatized gold colloids. The experimental points were recorded after standing for 20 min at each temperature.

Preparation of the Gold Substrates. Gold Colloids. Gold particles were prepared according to literature procedures.[35] Before use, all the glassware was washed with freshly prepared aqua regia (3:1 HCl:HNO_3) followed by extensive rinsing with doubly distilled water. Next, 39 mM sodium citrate (50 mL) was poured into boiling 1.0 mM $HAuCl_4$ (500 mL) under vigorous stirring. After the onset of a deep red color, boiling and stirring were continued for 15 min. The solution was cooled to room temperature under continuous stirring to yield a mother solution evaluated at 16 nM in colloid from UV/vis absorption,[36] by taking into account the average particle diameter of 12 ± 1 nm as determined by direct observation in transmission electronic microscopy (vide infra).

SPR Gold Plates. The BK7 glass slides used for SPR measurements were coated with thin films of titanium (1 nm, to increase the adhesion of gold) and gold (46 nm) by vacuum evaporation. These slides were cleaned immediately before use (1:1:5 H_2O_2:NH_4OH:H_2O) and rinsed with water. The slides were attached to the SPR prism via an index matching oil.

Derivatization of Gold Substrates. Typical Procedure for Polymer-Grafting of Gold Colloids. A mixture of 0.6 mg of the selected polymer **P** and 5 mL of a 16 nM solution of gold colloids was kept overnight at room temperature in the absence of light. In the case of the samples used for cloud point and TEM experiments, the derivatized gold colloids were purified by gel permeation chromatography over a Sephadex PD-10 prepacked column (Pharmacia). The resulting colloid fraction was either used immediately, or was lyophilized for storage. No difference in the behavior was noticed between the latter two types of samples during further experiments.

Polymer-Grafted Plates for SPR. The grafting process has been followed by SPR under continuous flow of polymer solutions at given concentrations. Weakly adsorbed polymer molecules were subsequently rinsed off by flowing water through the measurement chamber.

Derivation of the Affinity Constants $K(\mathbf{P})$ of the Polymers P for Gold Colloids. Absorbance data $A_\lambda([\mathbf{P}])$ were used to extract an order of magnitude of (i) the affinity constants $K(\mathbf{P})$ of the polymers **P** for the gold surface; and (ii) the change of the molar absorption coefficients of the gold colloids $\epsilon_\lambda(\infty)/\epsilon_\lambda(0)$ upon derivatization with the polymers. A two-state model similar to that of Langmuir to account for adsorption of a gas monolayer[37] was used to describe the association between the polymer molecules **P** and the gold colloids:

$$\mathbf{S_{free}} + \mathbf{P} = \mathbf{S_{bound}} \quad (4)$$

where every gold colloid (average radius $\mathscr{R}$) was assumed to contain $4\mathscr{R}^2/R(\mathbf{P})^2$ independent sites **S** for polymer anchoring, using the polymer radii $R(\mathbf{P})$ extracted from the preceding NMR experiments. The absorbance data were then analyzed from eq 5, which can be easily obtained:[38]

$$A_\lambda([\mathbf{P}]) = A_\lambda(0) - \frac{A_\lambda(0) - A_\lambda(\infty)}{2} \times \left\{\left(1 + x + \frac{1}{\mathscr{K}c_0}\right) - \left[\left(1 + x + \frac{1}{\mathscr{K}c_0}\right)^2 - 4x\right]^{1/2}\right\} \quad (5)$$

where $A_\lambda(0)$ and $A_\lambda(\infty)$ are the initial absorbance and the absorbance at full coverage of gold colloids, c_0 is the total molar concentration of the sites **S** (if C designates the molar concentration of the gold colloid, $c_0 = 4\mathscr{R}^2C/R(\mathbf{P})^2$), x is the ratio $[\mathbf{P}]_{tot}/c_0$ where $[\mathbf{P}]_{tot}$ is the total polymer molar concentration, and K is the affinity constant of the considered polymer for the occupation site **S**.

Dynamic Light Scattering. Light scattering measurements were done at 25 °C on 1−5 nM solutions of derivatized gold colloids after gel permeation chromatography. Incident irradiation at 514.5 nm was produced by a Coherent argon laser. A Brookhaven multiautocorrelator was used to generate the full autocorrelation function of the scattered intensity. The time correlation function was analyzed by a method of cumulants.

SPR Measurements. SPR measurements were performed at 293 K on a SPR-DEVI prototype (VTT, Tampere, Finland) with a diode laser (λ = 670 nm) as light source, angular resolution $f = 0.005°$.[39] Gold-coated slides were attached to the SPR prisms (BK7 glass, $n = 1.514$). The monochromatic light directed to a prism was reflected onto a photodiode. The intensity I of the reflected light was measured as a function of external incidence angle. Every experiment was computer

(33) de Gennes, P.-G. *Scaling Concepts in Polymer Physics*; Cornell University Press: Ithaca, NY, 1979.
(34) Jerschow, A.; Müller, N. *Macromolecules* **1998**, *31*, 6573−6578.
(35) Freeman, R. G.; Hommer, M. B.; Grabar, K. C.; Jackson, M. A.; Natan, M. J. *J. Phys. Chem.* **1996**, *100*, 718−724.
(36) (a) Brown, K. R.; Walter, D. G.; Natan, M. J. *Chem. Mater.* **2000**, *12*, 306−313. (b) Link, S.; El-Sayed, M. A. *J. Phys. Chem. B* **1999**, *103*, 4212−4217.
(37) Atkins, P. W. *Physical Chemistry*; Oxford University Press: New York, 1978.
(38) See, for instance: Jullien, L.; Canceill, J.; Valeur, B.; Bardez, E.; Lefèvre, J.-P.; Lehn, J.-M.; Marchi-Artzner, V.; Pansu, R. *J. Am. Chem. Soc.* **1996**, *118*, 5432−5442.
(39) Described on the Web site http://www.vtt.fi.

controlled. The change in δI at a fixed angle has been recorded during the experiments devoted to analyze the kinetics and the saturation of polymer adsorption. The thicknesses of the polymer films grafted on gold plates were estimated by applying the standard Fresnel equations, assuming refractive indexes equal to 1.566 as calculated from increments[40] for the polymers **P1** and **P1S**, and to 1.528 for the polymers **P2** and **P2S**, and dielectric constants, $\epsilon_{Ti} = -6.7126 + 19.855i$ and $\epsilon_{Au} = -13.869 + 0.8013i$ for the Ti and Au layer, respectively.

Aggregation Experiments. UV/vis absorption spectra were recorded over time after addition of 0.3 mL of 5 M aqueous NaCl to 2 mL of 4 nM solution of gold colloids to evidence any possible aggregation process. The final spectra were recorded after 3 h.

Tests for Evaluating the Unspecific Adsorption of Biomolecules by SPR. Bovine serum albumin, BSA (Sigma), solution with a concentration of 0.5 mg mL^{-1} and subsequently human serum (Jackson ImmunoReseach) were pumped into the measuring cell, and changes in the intensity of the light were detected for about 10−15 min at a fixed angle of incidence. The surface was rinsed with buffer between every injection of protein, and the amount of bound protein was determined. The polymer layer was also washed 30 min in a 1:1 cleaning solution of methanol:HCl 37% after adsorption of protein.

Etching Experiments. The absorption was monitored over time at 520 nm after addition of 90 μL of etching solution (1 mM $K_3[Fe(CN)_6]$, 100 mM of KCN[41]) in 2 mL of 4 nM gold colloids in a quartz cuvette. In the series of experiments devoted to complete gold coating after polymer grafting, 2 μL of 3-mercapto-1,2 propane diol (MPDiol) was added to the cuvette before etching of the polymer-coated gold colloids.

Electron Microscopy. Transmission electron microscopy (TEM) images were obtained with a Hitachi H-700H microscope operating at an acceleration voltage of 200 kV at a magnification of 200 000. Specimens of the various Au colloids were prepared by slow evaporation of a drop of the appropriately diluted solution deposited onto a collodium-coated copper mesh grid. The size distributions of the gold particles were measured from enlarged photographs of the TEM images.

Acknowledgment. The work was supported by the European Commission (research grants CEE BIO-CT97-962372). We are thankful to Dr. Hubert Hervet for his help during the dynamic light scattering experiments.

Supporting Information Available: SPR spectra, absorption spectra, and TEM images (PDF). This material is available free of charge via the Internet at http://pubs.acs.org.

JA010796H

(40) van Krevelen, D. W. *Properties of polymers*, 3rd ed.; Elsevier: Amsterdam, 1990; pp 290−297.

(41) Marikanos, S. M.; Novak, J. P.; Brousseau, L. C., III; House, A. B.; Edeki, E. M.; Feldhaus, J. C.; Feldheim, D. L. *J. Am. Chem. Soc.* **1999**, *121*, 8518−8522.